AD-A047 422 CIVIL ENGINEERING LAB (NAVY) PORT HUENEME CALIF F/G 20/11
FRACTURE TESTS WITH AN ELECTROHYDRAULIC PULSER.(U)
DEC 76 T A SHUGAR, R J ODELLO
UNCLASSIFIED CEL-TM-51-76-19 NL

1 OF 1
ADA047 422

END
DATE FILMED
1-78
DDC

TM no. (14) CEL-TM-51-76-19

(1)

TECHNICAL MEMORANDUM

title: (6) FRACTURE TESTS WITH AN ELECTROHYDRAULIC PULSER.

author: (10) Theodore A. Shugar [redacted] Robert J. Odello

date: (11) Dec [redacted] 76 (12) 29p.

(9) Technical memo.,

sponsor: DEFENSE NUCLEAR AGENCY - Subtask Y99QAXSC318 Ground Motion Effects on Underground Structural Systems and Contents, Work Unit 05 Experimental and Analytical Development in Structural Dynamic Response

program nos: (16) F008-08-02-108 Y99QAXS (17) YF008802, C318

CIVIL ENGINEERING LABORATORY
NAVAL CONSTRUCTION BATTALION CENTER
Port Hueneme, California 93043

391 111

CONTENTS

INTRODUCTION

Objective

The overall goal of this effort was to produce spall fractures at the outer surface of hydrostone specimens to demonstrate that an electrohydraulic spark can be used as a stress wave source for fracturing brittle materials, ~~as described in Reference 1~~. The immediate objective of this study was to demonstrate that electrohydraulic blast loading could produce fracture in hydrostone specimens.

Scope

This study was primarily an experimental effort with limited goals. Electronic instrumentation for measuring stress magnitude and duration was not used because of the difficulties encountered with such measurements during the efforts described in Reference 2. The presence or absence of failures and descriptions of failure surfaces were the primary sources of data. The nature of the fracture mode and of the electrohydraulic discharge were inferred from these observations.

Time and cost constraints dictated the use of existing electrohydraulic equipment at the Civil Engineering Laboratory (CEL). Minor modifications to the equipment and its setup are described later in this report. Minor changes in the power head are also described.

Although the basic goal of this effort was to study the effects of stress waves in a brittle solid, a limited analysis of the electrohydraulic circuitry was performed to determine if the equipment h[illegible] capabilities to produce the desired stress waves. Potential s[illegible] of energy losses and potential discharge rates were estimated. [illegible]r modifications of the electronic circuitry were not attempted.

Background

The ultimate goal toward which this study is directed is the development of an efficient high-speed tunneling method for hard rock media. Present automated methods for tunneling in hard rock become less effective as rock compressive strength increases. The proposed method fails the rock in tension, and is thus more effective for hard, brittle materials. It consists of cutting a circular kerf or trepan at a diameter equal to that of the tunnel. A small diameter hole is then drilled concentric with the trepan and high magnitude, short duration stress pulses are created in the smaller hole. These divergent, compressive stress pulses propagate outward to the free surface of the

cylinder created by the trepanning where they are reflected as convergent tensile stress pulses and fail the rock in tension. The method has the advantage of breaking rock in its weakest mode and using a small amount of energy per unit volume of rock removed.

The rock breaking technique was initially demonstrated by detonating small explosive charges in hydrostone cylinders[1]. The success of these initial efforts led to the procurement of an electrohydraulic power supply and power head that would have the capability for breaking rock specimens on the order of 1/3 to 1/2 metre in diameter. Tests on the rock specimens indicated that the equipment did not deliver enough power to the rock[2] to cause fracture. Calculations indicated that the equipment would be capable of spalling hydrostone.

Reference 2 therefore recommended that a circuit analysis be conducted to determine how the present electrohydraulic system might be improved. Further, it recommended that test specimens of hydrostone be employed to determine whether fractures similar to those reported in Reference 1 for hydrostone specimens and chemical explosives could be achieved.

PHASE I EXPERIMENTS

Test Specimens

A total of four hydrostone specimens were fabricated for the initial demonstration tests with the electrohydraulic pulser system. The geometrical configuration and properties of the specimens are presented in Figure 1 and Table 1, respectively.

Experimental Setup

The test setup and electrohydraulic power head are shown in Figures 2 and 3, respectively. Primary features of this system are the control console which produces a d.c. voltage of up to 17 KV, a rectifier unit, a capacitor bank with a total capacitance of 45 μf, and a power head which produces a spark across its electrodes where the capacitor bank is discharged.[3]

The control console contains all of the power, control relays and switches necessary for start-up control, energy level selection, firing sequence and shutdown of the 5 kilojoule power supply. Single phase, 220 volt power is brought to the control console where it is reduced to 120 v for control power.

The rectifier unit contains a high voltage pole transformer, a full wave bridge rectifier, charging resistors and a forced air cooling system. Input voltage to the transformer is stepped up by a ratio of 65 to 1, rectified and applied to the capacitor bank unit through current limiting charging resistors. A single RG8AU cable carries high voltage d.c. to the capacitor bank unit.

The capacitor bank unit contains 6, 7.5 μf, high-frequency discharge capacitors which are connected in parallel to produce a total bank capacity of 45 μf. Included in this unit is the switching ignitron and its associated trigger unit. A fail-safe, gravity drop instant discharge switch is also located within the cubical. Ten parallel RG8AU coaxial cables carry the pulse power from the igniton to the external load, which, in this case, is a spark gap within a contained liquid.

The electrohydraulic power head primarily consists of two electrodes which are separated by a hollow, thick-walled cylindrical insulator. The hot lead from the ignitron attaches to the top electrode of the power head and the ground lead attaches to the base electrode. The entire assembly is placed atop the test specimen and clamped in place by a steel channel and tie-rod assembly.

A liquid, either deionized water or a cupric sulfate solution, is poured into the 50mm (2 in.) diameter hole prior to placement of the power head assembly. Later additional liquid is added through a hole in the power head assembly which intersects the liquid chamber slightly above the spark gap. A socket head cap screw provides a seal for this filler hole. Thus, the entire enclosed volume is filled with liquid. A flexible liner is employed to contain the liquid and prevent it from seeping into the pourous hydrostone.

Results

The first attempts at fracturing a hydrostone specimen were not successful. The specimen originally possessed a hole depth of 150mm (6 in.). The hole was backfilled to the 50mm (2 in.) depth shown in Figure 1.and again tested using maximum voltage without success.

It was postulated that the flexible liner or rubber bladder between the liquid and the hydrostone was absorbing too much energy due to its compressibility. It was removed, and the hole was coated with a leakproof epoxy to prevent seepage into the specimen.

The next attempt at fracturing the hydrostone specimen was successful. It too was made at maximum voltage. Working without the bladder presented a problem in creating a pressure seal, but this was overcome with a greased rubber gasket sandwiched between the plate of the power head and the hydrostone specimen. The clamping forces which are normally applied to the power head and specimen compress the gasket and provide an adequate pressure seal. The three remaining specimens were successively fractured with the bladderless configuration.

The four fractured test specimens are shown in Figure 4. All the fracture modes were characterized by radial cracks, exclusive of desirous spall crack (circumferential) failure. These results demonstrated that while the electrohydraulic pulser was capable of fracturing test specimens, the fracture damage was neither sufficiently rigorous nor of the desired mode. It was believed that the stress wave produced by the electrohydraulic pulser would produce fractures similar to those reported in Reference 1 where chemical explosives were employed with hydrostone specimens.

Energy Calculations

An energy comparison between the two methods was made to ascertain whether the electrohydraulic method and the chemical explosive method were comparable in potential energy. The applicable electrohydraulic system parameters are 45 microfarads capacitance at 17,000 volts. Then the potential energy for the system is $1/2\ CV^2$ where C is the capacitance and V is the voltage; or 6,500 joules of stored energy. The series C and D hydrostone cylinders of Reference 1 corresponded closely in size and shape with the present cylinders (Figure 1). All these cylinders (a total of five) were fractured with a stress wave produced by lengths of detonating cord explosive (PETN) detonated in the holes at the top of the cylinders. These tests are summarized in Table 2. Energy equivalance was based on the data of Reference 4. All five cylinders sustained both radial and spall (circumferential) fracture surfaces and sustained damage far more extensive than that shown in Figure 4.

From this comparison it is concluded that the electrohydraulic pulser stores sufficient energy to create more fracture damage than what has been demonstrated thus far. The pulser stores as much as 6,500 joules and this energy, when released, has produced radial crack failures exclusive of spall cracks and only moderate amounts of damage. The chemical explosive tests demonstrated that both radial and spall failures can be achieved in similar hydrostone specimens with anywhere from 2,250 joules to 10,700 joules of stored energy. Improvements in system efficiency and pulse shape characteristics are indicated as a result of these calculations.

IMPROVEMENTS TO THE ELECTROHYDRAULIC PULSER

Modifications

It was apparent that the total potential energy stored in the capacitor bank was not being delivered to the specimen in an optimal manner upon release of the ignitron trigger. Initially it was thought that the problem was an impedance mismatch between the load (submerged spark gap) and the RG8AU transmission cable. Such a condition could indeed extract energy from the system. However, the ignitron rise time is 1/2 microsecond, and though this appears fast, it is enough time for the current to reach the load and to return to the ignitron. Therefore in a circuit analysis, the transmission cable can be eliminated as an element with regard to the question of impedance mismatch.

The cable resistance itself is another potential source of energy loss. It was decided to remove these cables and to modify the test setup so that the capacitor bank unit is in the test bay adjacent to the power head assembly. In this way 12m (40 ft) of RG8AU cable were replaced by 0.6m (2 ft) of braided copper strap.

No modifications to the power head assembly were made to improve its efficiency, although some ideas were advanced. It is believed that if the power head were modified so the electrodes were placed directly into the hole in the specimen, a more efficient transfer of energy could be achieved. Such a modification would have involved more effort than could be justified by the scope of the project because the power head was fabricated from a special steel which could not be machined with normal procedures. A simple solution would be to machine a circular flat plate to accept a standard spark plug and to fit the existing hold-down apparatus. The single plate could replace most of the power head assembly, and when bolted in place would position the spark plug gap just below the specimen's top surface. However, it is not certain whether a standard spark plug could produce the desired electrohydraulic effect or whether it could withstand the severe shock environment.

System Circuit Analysis

A circuit analysis of the electrohydraulic system was conducted and both voltage and current data were obtained by appropriate measurements. These efforts are described in the Appendix. The basic findings were:

1. The circuit is an underdamped system; therefore it may not be ideal for creating a minimum duration pulse. Such a system would have to be critically damped according to linear theory.

2. Discharge voltage measurements were made with a high voltage probe and recorded on an oscilloscope. A peak current of 49,000 amps at the load gap was computed using the measured voltage. This current is more than sufficient for the task at hand. The auxillary analysis was based on the equation for the underdamped solution.

3. Direct measurements of the current were made with the in-line shunt method to verify the above calculation. These measurements indicated a peak current of 300,000 amps but were not considered as reliable as the voltage measurements. A subsequent circuit analysis was made to account for this seemingly high current. However, only partial success was achieved in explaining the difference. In the end, the direct current measurements were discarded and the figure of 49,000 amps was considered accurate.

PHASE II EXPERIMENTS

Three additional hydrostone test specimens, of the same size as before, were processed for testing with the modified electrohydraulic pulser system. The only changes to the system were a deletion of the lengthy transmission cable between the capacitor bank unit and the power head, and placement of this unit in the test bay immediately

adjacent to the power head specimen setup. No changes to the power head assembly were made except that the bladderless configuration was still employed.

Results

Upon the first few attempts at fracturing the specimens, the pressure seal or gasket failed dramatically with liquid being blown against the test bay walls. No concommittant failure of the specimens occurred. Since this had not happened previously, it was taken as an indication that the efficiency of the electrohydraulic system was improved appreciably. A metal retainer was fashioned to fit around the rubber gasket and prevent the gasket from distorting and moving laterally. Upon resumption of the tests, no pressure seal failures occurred and extensive fractures were achieved.

The fractured test specimens, numbered 5 through 7, are shown in Figure 5. By comparing these failures, especially that of number 5, with the previous failures, it is apparent that more energy is being delivered to the test specimens. The extent of fracture in specimens 5 through 7 exceeds that which was seen in the previous four specimens.

The hole depth was successively increased from 50mm (2 in.) to 150mm (6 in.), and finally to 300mm (12 in.) to obtain a fracture behavior pattern associated with the hole depth parameter. In these hydrostone specimens the depth of the hole apparently controls the depth of radial fracture surfaces. As can be seen clearly in specimens 6 and 7 the radial fracture surface extends to the bottom of the hole. The fracture surface then changes to a tangential surface further down in the specimen. A transitional fracture zone separates the two types of fractured surfaces.

The tangential fractures shown in Figure 5 are reminiscent of the circumferential spall fractures obtained in Reference 1, but are not the same. True circumferential spall fractures occur on a cylindrical surface, symmetrical about the specimen axis. Therefore, true circumferential fractures are rotationally symmetric and tend to reduce the cylindrical specimen diameter. By contrast, tangential fractures are not rotationally symmetric and tend to "square" the cylindrical specimen.

Throughout the project it was curiously evident that the radial crack pattern, when viewed from above the cylinder, generally divided the cylinder into either equal quadrants, equal thirds, or equal halves. This uniformity can be seen in the fracture pattern of all specimens, with the possible exception of number 5. These remarkably well defined and reproducible fracture patterns are due neither to the geometry nor the positioning of the power head onto the specimen, but rather due to a characteristic of impulsive loading. Random fracturing, which must be treated statistically, frequently occurs under static loading. But for impulsive loading, the rather even distribution and reproducibility of crack patterns is inherent and based upon the stress relief region that instantly develops around a crack tip while the crack is being formed.

Discussion of Fractures

Though the fractures depicted in Figure 5 are extensive, the mode of fracture is still dominated by radial cracks. In an attempt to determine why these results are different from those presented in Reference 1 where circumferential cracking was also present, the following discussion is given. A thorough analytical investigation was beyond the scope of the project.

There are several possible explanations for the differences in behavior between the specimens loaded with detonating cord explosives and those loaded by the electrohydraulic pulser:

Stress wave geometry
Pulse duration
Hole geometry
Other factors

Each of these factors will be discussed individually in the following paragraphs.

1. Stress Wave Geometry. In the initial tests, detonating cord was placed along the axis of the cylindrical hole for its full length. The cord was detonated at the end that was protruding from the hole, and the detonation progressed along the axis of the hole at a speed of approximately 7,900 m/sec (26,000 ft/sec). Thus, the wall of the hole in the test specimen experienced a pressure wave front that moved at about the detonation speed of the explosive. In the present tests, the detonation source was located outside of the hole and above the specimen. The initial shape of the shock front was that which would emanate from a point source due to the electrode configuration, and would be more or less spherical by the time it arrived at the top of the hole. The stress wave propagated through the liquid at a speed of only about 1,500 m/sec (4,800 ft/sec); therefore, the stress wave in the hydrostone which traveled at about 2,800 m/sec (9,300 ft/sec) tended to outrun the wave from the loading source.

An important consequence of the difference in geometry of the stress wave propagation for these two tests is that the dilatation wave does not strike the free surface of the cylinder at normal incidence. Based on the above stress wave velocities, Figure 6 shows the approximate, computed positions of the shock fronts as they impinge on the free surface for each test configuration. In the present tests, the angle of incidence was approximately 68^{o}, while in the tests with detonating cord the angle was approximately 20^{o}, or more nearly normal. From the equations in Reference 5, the relative magnitudes of the reflected tensile wave with respect to the impinging compression wave are approximately 0.9 and 0.4, respectively. Thus the tests with the present power head configuration are not likely to produce circumferential spalls because the tensile wave is of much lower magnitude than the compression wave. The resulting stress wave interaction probably does not provide an area of sufficiently high net tensile stress to produce spalling.

Two tests were conducted to determine the effect of having a more or less linear spark discharge within the hole. The objective was to produce a normally incident stress wave. A 50mm (2 in.) diameter hole was drilled the full depth of each specimen. Steel rods, 3.2mm (1/8 in.) in diameter, were welded to electrode plates and inserted into the holes to create a 75mm (3 in.) linear spark gap. The holes were filled with deionized water. In both tests the specimens failed along radial lines with no evidence of circumferential spalls. Figure 7 shows the fractured test specimens and the electrodes. Here again it is seen that the radial fractures extend to the depth of the hole and the impulsive loading results in a rather uniform bisection and trisection of specimens 8 and 9, respectively.

2. Pulse Duration. The test results and circuit analysis both indicate that the stress pulse duration for the pulser tests was much longer than for the detonating cord tests. The measured pulse duration for the electrohydraulic system was 40 μ sec, while the estimated duration of the blast pulse from the detonating cord was only 10 μ sec. In the two tests in which the spark was initiated along the axis of a hole running the entire length of the specimen, only radial cracks were formed. So even when the stress wave is permitted to approach the free surface at a normal angle, the pulse duration is too long to produce a net tensile pulse of sufficient strength to cause spalling. The failure mode shown in Figure 7 is more characteristic of static failure than stress wave fracturing.

3. Hole Geometry. In the tests using chemical explosives the hole bottoms were hemispherical, but the hole bottoms in the present investigation were relatively flat with small radii of curvature at the transition. In Reference 6 it was shown that under static loading, meridial stresses can be as much as 50% greater in holes with flat ends compared to those with hemispherical ends. In the former case stress concentrations occur in the transition area between the wall and the hole end. The transition zone fracture pattern as is evident in Figure 5 is consistent with high meridial stresses. These stress concentrations lead to the development and propagation of unwanted cracks that dissipate most of the pulse energy. Thus the hole geometry could have contributed to a deterioration of the stress pulse. On the other hand, static and impulsive loads produce fracture modes which are very different, so the hole geometry factor based on static loading may not be significant for impulse loads.

4. Other Factors. With the detonating cord configuration, no axial preload was required on the cylindrical specimen. However, the power head, in the electrohydraulic system, must be held in place and the pressure seal must be maintained with a certain amount of compression. Thus the tie-rods (Figure 2) introduce an axial preload into the specimen when testing with the electrohydraulic pulser.

Expanding gas released with the primacord explosive may contribute to crack propagation whereas no such augmentation of the fracture pro-

cess exists with the electrohydraulic pulser. But it is unlikely that expanding gas could do a significant amount of work when it is not completely confined within the specimen hole. This factor is probably negligible.

SUMMARY

Initial experiments with an electrohydraulic pulser system and hydrostone test specimens achieved only minor fractures in the specimens. These preliminary results were obtained only after removal of a rubber bladder between the liquid pressure medium and the hydrostone surface. It was believed that this component was absorbing sufficient energy to prevent the resulting stress wave in the hydrostone from reaching a fracture-level intensity.

Calculations of the potential energy capacity of the electrohydraulic pulser system revealed that the system possessed an amount of energy comparable to that which was also calculated for previous successful fracture experiments using detonating cord explosives and similar test specimens.

Modification of the electrohydraulic pulser system was undertaken to improve its efficiency in delivering energy to the spark gap and to the test specimen. The basic modification resulted in removal of approximately 12 metres (40 ft) of signal cable, with its associated electrical resistance, between the capacitor bank and the power head. This necessitated placing the capacitor bank unit in the test bay adjacent to the power head-test specimen location.

Resumption of the experimental fracture tests with the modified system produced fractures which were obviously more extensive than those achieved with the pulser system in the initial experiments. Further, from visual inspection, the fractures were comparable in extent, though not mode, to those from the previous detonating cord experiments thus corroborating the implied equivalence of the two methods in producing stress waves possessing similar energy levels.

Various explanations were offered in an attempt to account for the inability of the electrohydraulic pulser system to produce fracture patterns which include true circumferential type failures (scabbing, spall). Most likely this was due to either one or both of the following reasons. First, the electrohydraulic pulser system produces a very confined spark which is nearly a point source and which tends to produce a spherical wave propagating into a cylindrical medium. Such a wave is not as conducive to scabbing as a cylindrical wave which is both incident and reflected in a normal direction with the free cylindrical surface of the test specimen. Secondly, the duration of the discharge across the spark gap electrodes was suspected as being too long. Discharge voltage measurements indicated that the duration was approximately four times longer than that achieved in the detonating cord experiments. A faster discharge results in a higher intensity, less diffuse, stress wave at constant energy levels.

CONCLUSIONS

The tests and analysis reported herein have led to the following conclusions with respect to the use of electrohydraulic equipment for producing controlled stress waves in a brittle material.

1. Polyurethane or other relatively soft liners cause a reduction in the stress wave energy transmitted to the specimens.

2. Long transmission cables between the capacitor bank and the spark gap significantly reduce the electrohydraulic discharge energy.

3. If energy losses are minimized, the present CEL electrohydraulic equipment can produce fracturing in hydrostone specimens.

4. The present electronic and physical configuration of the CEL electrohydraulic equipment does not produce stress pulses of the proper shape and orientation to produce circumferential spalls in the specimens.

RECOMMENDATIONS

Although the ultimate goal of this study, the demonstration of circumferential spalling with electrohydraulic stress pulses, was not achieved significant progress was made. Further efforts should be directed toward modifying the power head and electronics configuration of the electrohydraulic pulser to create the desired stress pulse shape in the specimens. If this can be achieved and circumferential spalls can be produced with the electrohydraulic effect as a stress source, a series of tests should be conducted to determine the input energy required to spall rock with this method. This approach will permit a quantification of the energy requirements of this concept for rock excavation.

ACKNOWLEDGEMENTS

Appreciation is expressed to Mr. Jim Brooks for his cooperation in conducting the circuit analysis and voltage measurements and for his expert consultation. Mr. Vince Gerwe was instrumental in setting up and conducting the electrohydraulic pulser tests in a timely fashion.

REFERENCES

1. Civil Engineering Laboratory. Technical Note N-1184: Comminution of rock with controlled stress waves, by R.N. Murtha, R.J. Odello, and J.R. Allgood, NCBC, Port Hueneme, CA, Oct 1971.

2. _____. Technical Note N-1432: Rock spalling through electrohydraulics, by R.J. Odello, NCBC, Port Hueneme, CA, April 1976.

3. Anonymous. Instruction manual for 5 kilojoule pulsed power supply. (SA-3001A-147) Environment/One Corporation. Schenectady, NY, Oct 1973.

4. Department of the Army Technical Manual TM9-1910: Military explosives. Washington, DC, April 1955.

5. H. Kolsky. Stress waves in solids. Dover Publications, Inc., New York, 1963.

6. W.F. Riley and A.J. Durelli. "Boundary stresses at the ends of pressurized cylindrical holes axially located in a large cylinder," Proc. Society for Experimental Stress Analysis, Vol. 17, No. 1, Jan 1959, pp 115-126.

Table 1. Approximate Mechanical & Physical Properties of Hydrostone (From Reference 1).

	S.I.	English
density, ρ	1620 Kg/m^3	101 lb/ft^3
static compressive strength, f_c'	35.2 MPa	5,100 psi
tangent modulus at 50% f_c'	8,240 MPa	1.2×10^6 psi
Poisson's ratio, ν	0.35	0.35
sonic velocity, c_1	2,850 m/sec	9,340 ft/sec

Table 2. Geometry and computed energy for Series C and D tests in (Reference 1).

Specimen[a] No.	Hole Diameter mm	(in)	Charge PETN grains	No.[b] Shots	Energy Per[c] Shot Joules
C1	50	(2)	13	1	6,970
	50	(2)	20	1	10,700
C2	63	(2.5)	5	2	2,680
C3	120	(4.75)	16	2	8,580
D1	50	(2)	4.2	4	2,250
D2	50	(2)	4.2	3	2,250

Notes: [a] All Specimens were 300mm (12 in.) diameter by 600mm (24 in.) tall.

[b] Multiple charges were used to demonstrate a capability for successively fracturing the specimens.

[c] Based on 536 Joules/grain PETN (Reference 3).

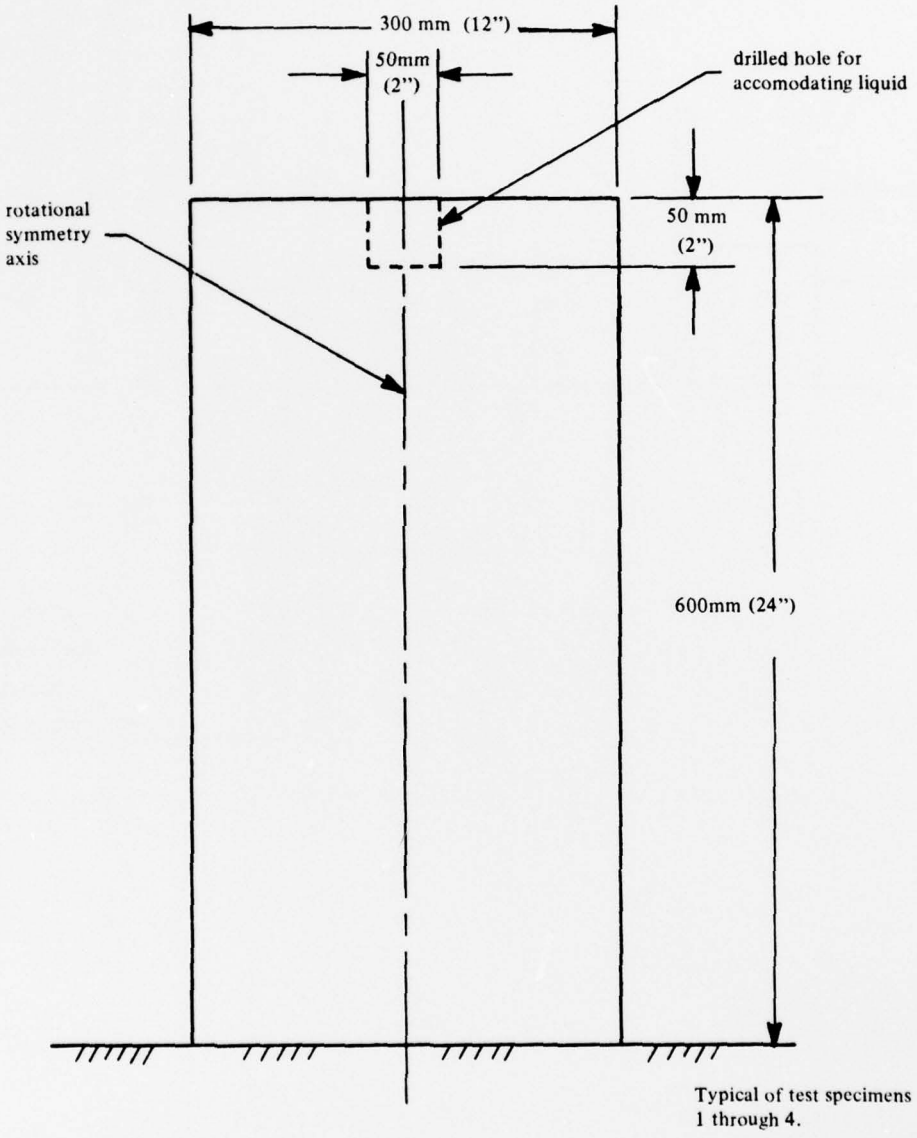

Figure 1. Hydrostone Cylinder Configuration

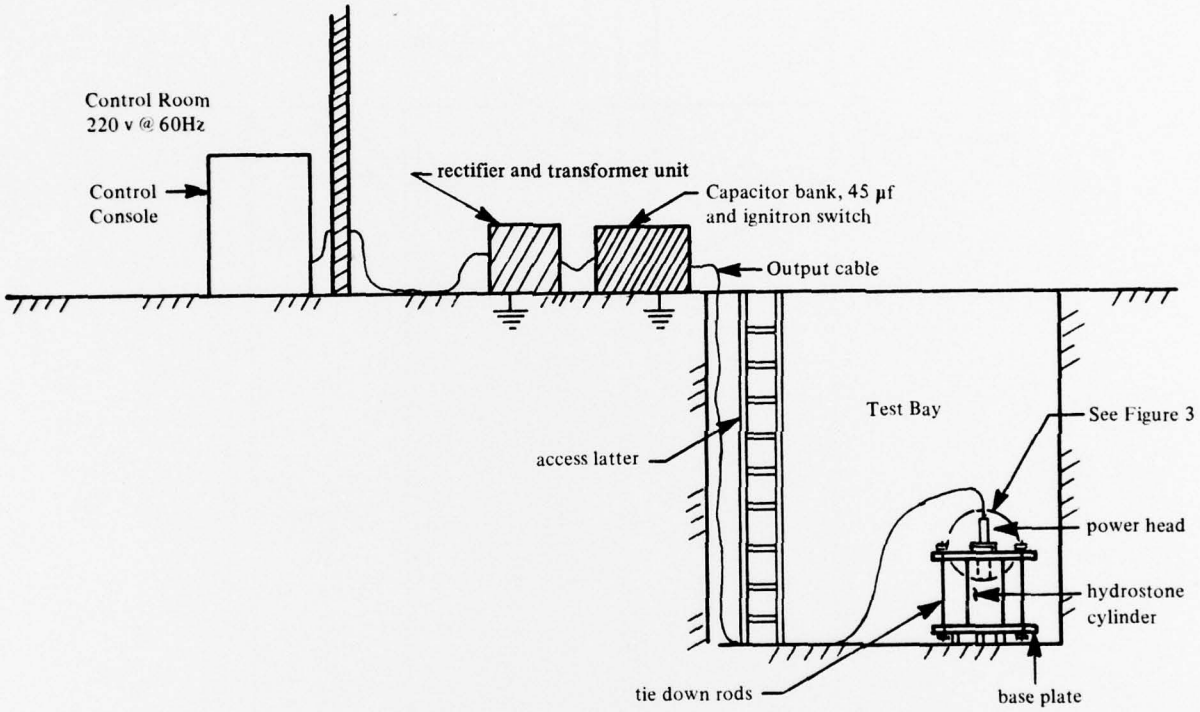

Figure 2. Physical Test Facility

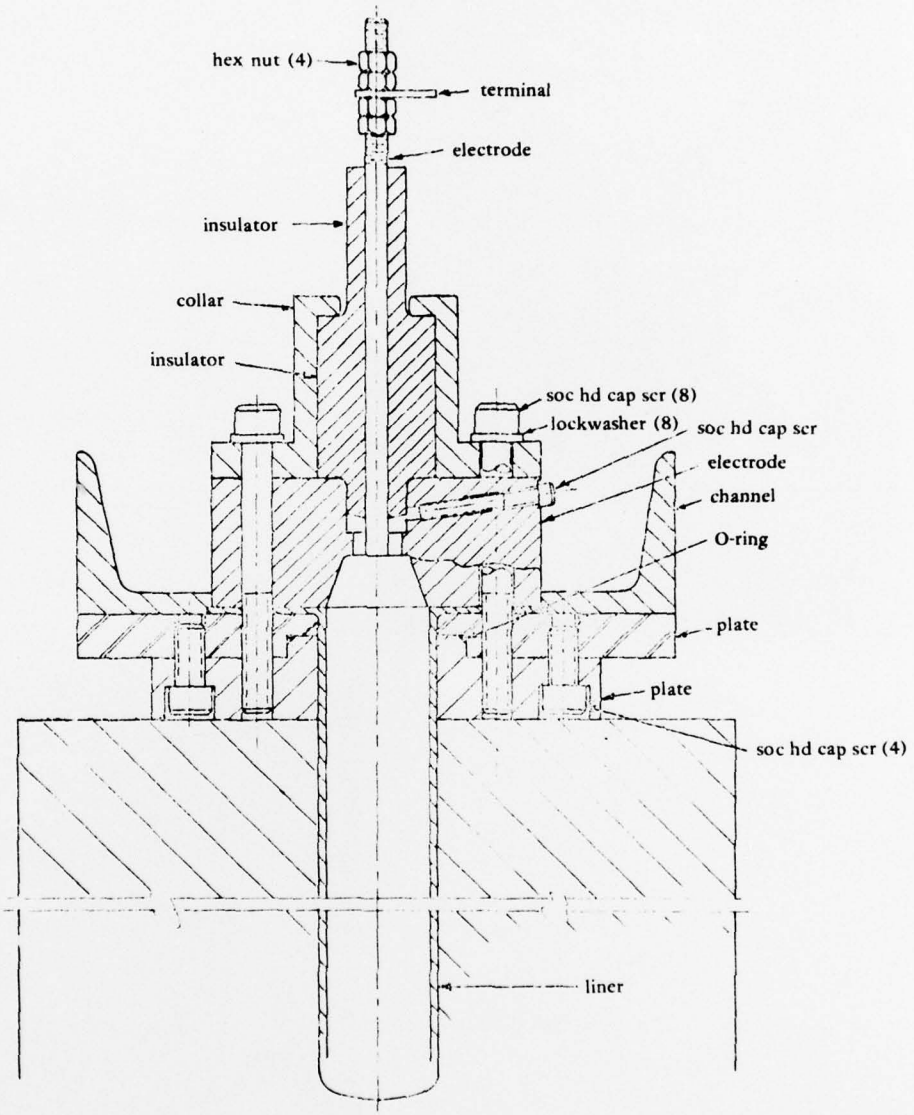

Figure 3. Cross section of electrohydraulic power head.

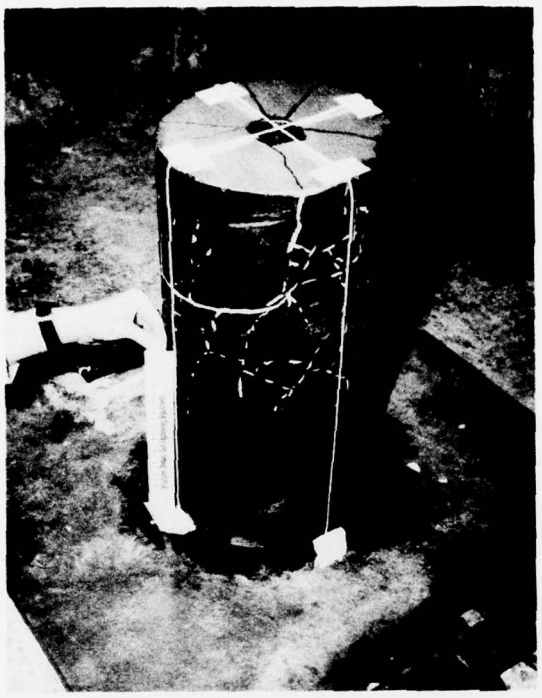

Specimen #1

Specimen #2

Figure 4. Fractured Hydrostone Specimens-Initial Experiments

Specimen #3

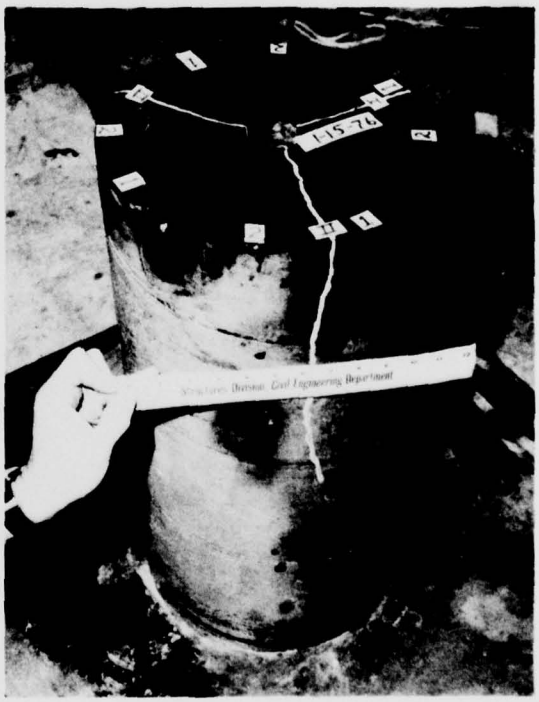

Specimen #4

Figure 4. cont'd Fractured Hydrostone Specimens-Initial Experiments

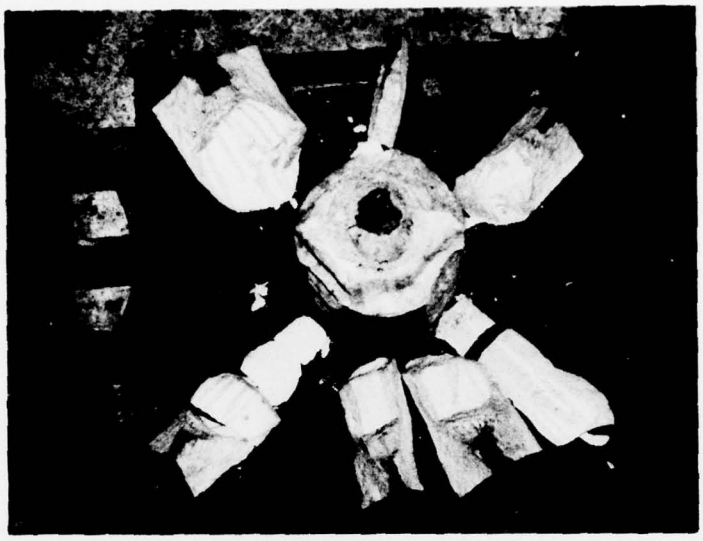

Specimen #5
2" deep hole

Specimen #6
6"deep hole

Figure 5. Fractured Hydrostone Specimens-Improved Pulser

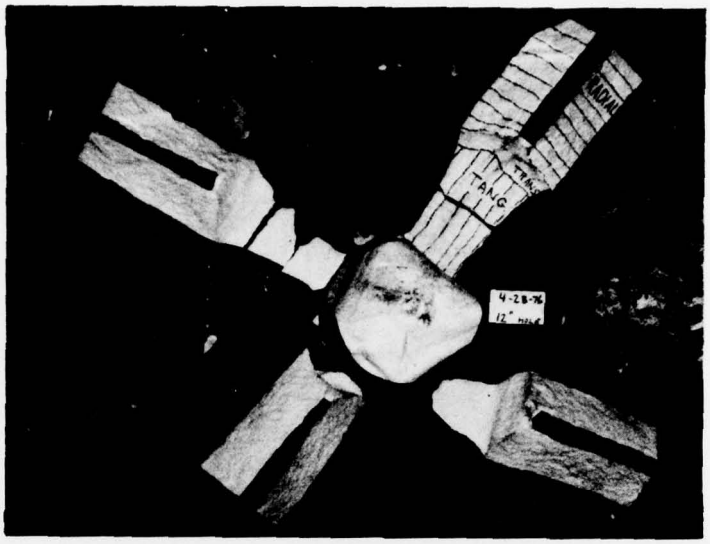

Specimen #7
12" deep hole

Figure 5. cont'd Fractured Hydrostone Specimens-Improved Pulser

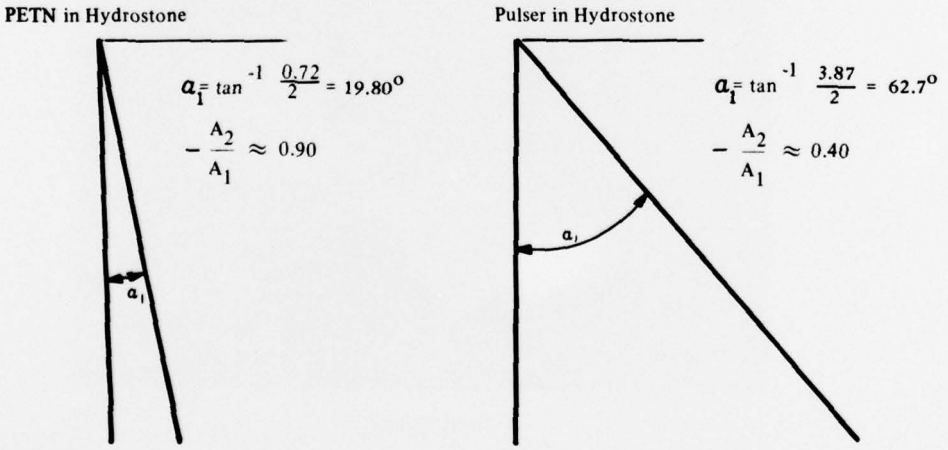

Figure 6. Shock Front Comparisons

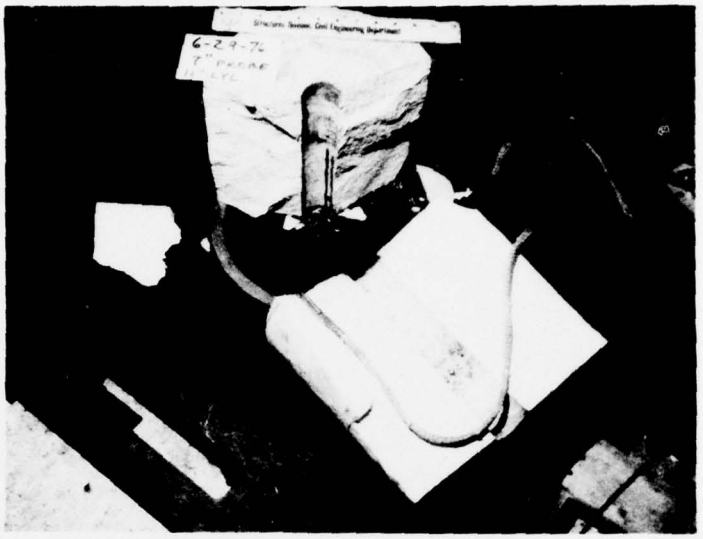

Specimen #8

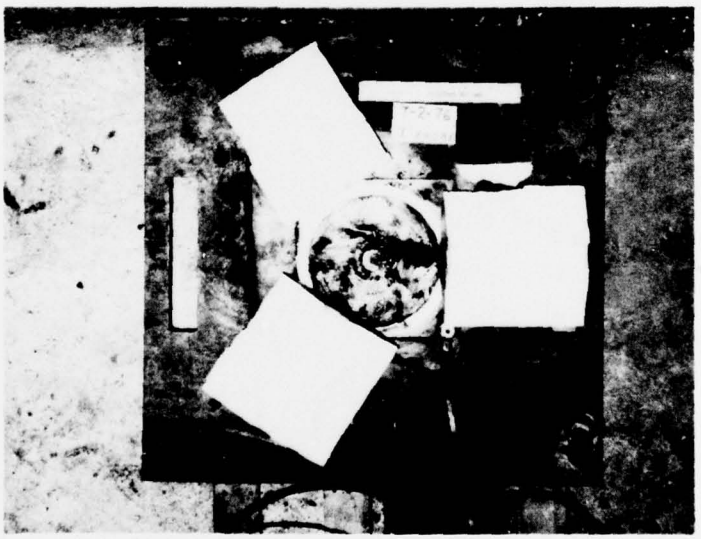

Specimen #9

Figure 7. Fractured Hydrostone Specimens-Linear Source

APPENDIX A

CIRCUIT ANALYSIS AND VOLTAGE MEASUREMENTS

by

James L. Brooks

Circuit Analysis

The electrohydraulic discharge apparatus is basically an RLC circuit as illustrated in Figure A-1. The governing equations for this circuit are:

$$e_C + e_R + e_L = o \tag{A-1}$$

$$e_C = \int \frac{i\,dt}{C} \tag{A-2}$$

$$e_R = iR \tag{A-3}$$

$$e_L = L \frac{di}{dt} \tag{A-4}$$

where e_C = voltage across the capacitance

e_R = voltage across the resistance

e_L = voltage across the inductance

i = current

t = time variable

R = resistance

L = inductance

C = capacitance

Substituting equations A-2 to A-4 into equation A-1 and differentiating with respect to time gives

$$\frac{i}{C} + L \frac{d^2 i}{dt^2} + R \frac{di}{de} = o \tag{A-5}$$

This is a second order linear differential equation whose solution can be expressed as

$$i = Ie^{kt} \tag{A-6}$$

$$\text{where } K = \frac{-R}{2L} \pm \sqrt{\frac{R^2}{4L^2} - \frac{1}{LC}} \tag{A-7}$$

Additional boundary conditions are necessary to determine the value of I.

The value of K is the critical parameter in determining the characteristics of the discharge circuit. For real values of K ($R > 2\sqrt{L/C}$). the circuit is overdamped. When K is a minimum ($R = 2\sqrt{L/C}$) the circuit is critically damped, and if K is complex ($R < 2\sqrt{L/C}$) the circuit is underdamped. Current-time histories for each of these conditions are shown in Figure A-2.

Voltage Measurements

The high voltage pulser used in the investigation described in this report was purchased from Environment One Corporation. The manufacturer's ratings for the equipment were:

Maximum voltage	-	17,000 volts D.C.
Total capacitance	-	45 μf
Input power	-	25 KVA at 220 v, 60Hz, single phase

The basic circuit diagram for the system is shown in Figure A-3.

The voltage measurements were designed to provide a measure of the system output under discharge conditions. Two carbon blocks which were set 0.5 mm (0.02 in.) apart to form an air gap were used as the load resistance for these measurements. With the exception of the load resistance the physical and electronic setup for these measurements was the same as that used in the Phase I experiments. Specifically, the 12 metre (40 ft) length of output cable was used between the capacitor bank and the load. A high voltage probe was connected to the output of the capacitor bank (point A in Figure A-3). The capacitors were charged to 10 KV as indicated on the voltmeter at the control console.

Typical oscilloscope records of the voltage probe output are shown in Figures A-4 and A-5. These time-histories clearly indicate an underdamped circuit, for which the following equations can be derived:

$$\frac{e_2}{e_1} = e^{-\frac{RT}{4L}} \qquad \text{(A-8)}$$

$$L = \frac{T}{4\pi^2 C} \qquad \text{(A-9)}$$

$$I = 1.57\, C \frac{de}{dt} \qquad \text{(A-10)}$$

where e_1, e_2 = first and second voltage peaks respectively

T = period of oscillation

de = change in capacitor voltage during time dt

dt = time for capacitor voltage to change from maximum positive value to maximum negative value.

Scaling data from Figures A-4 and A-5 indicates that the measurement circuit has an equivalent inductance of 1.3 μh and a resistance of 0.055 Ω. The peak current is thus 49,000 amps.

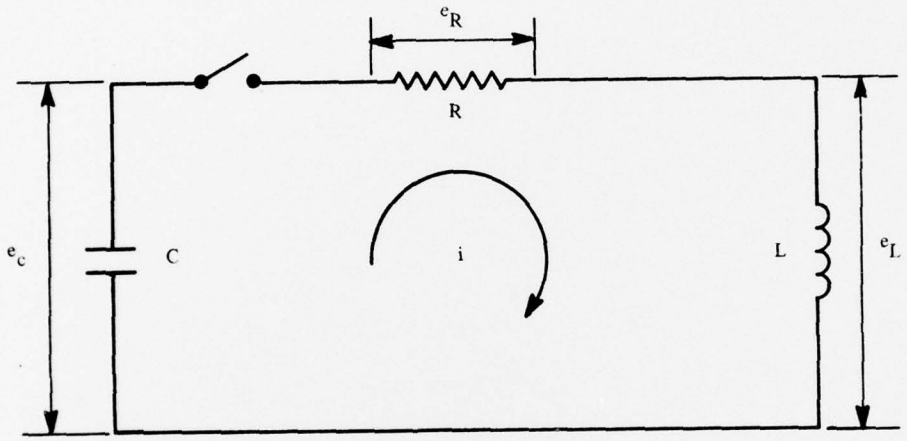

Figure A-1 Typical RLC circuit

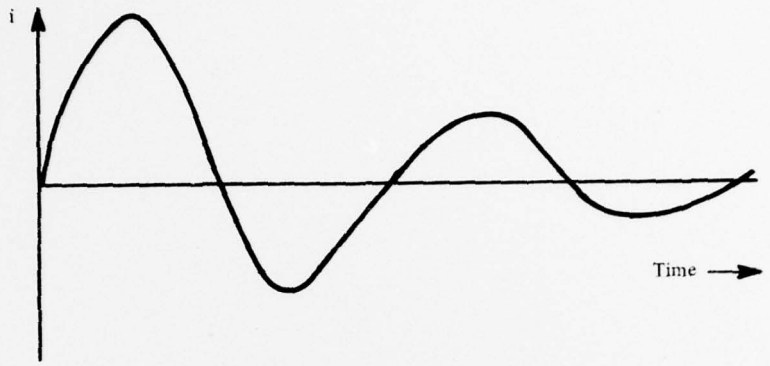

Under Damped

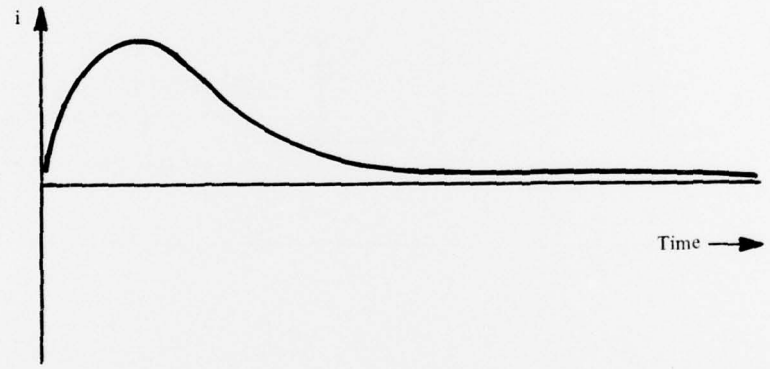

Critically Damped

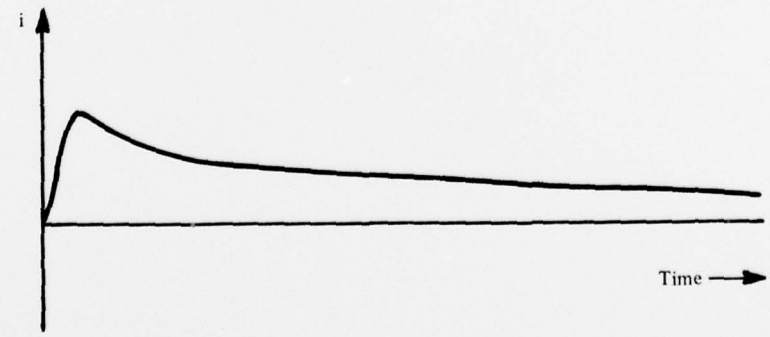

Over Damped

Figure A-2 RLC circuit current-time histories

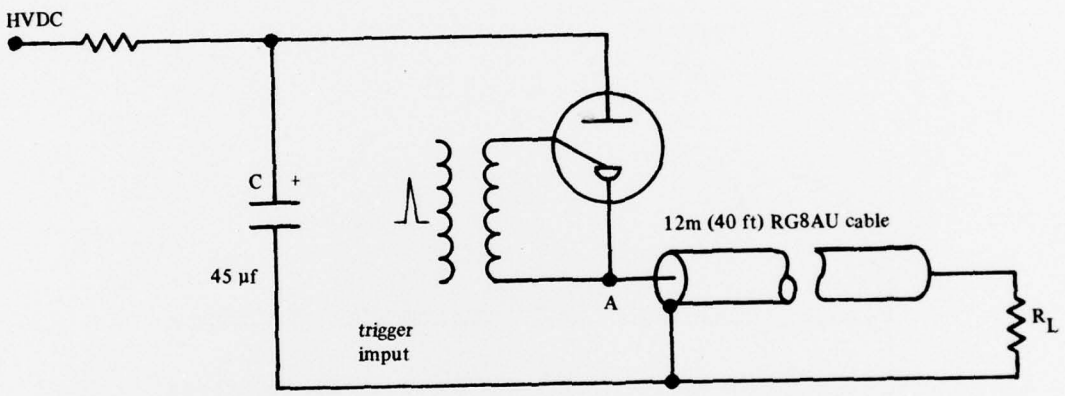

Figure A-3 Basic pulser circuit

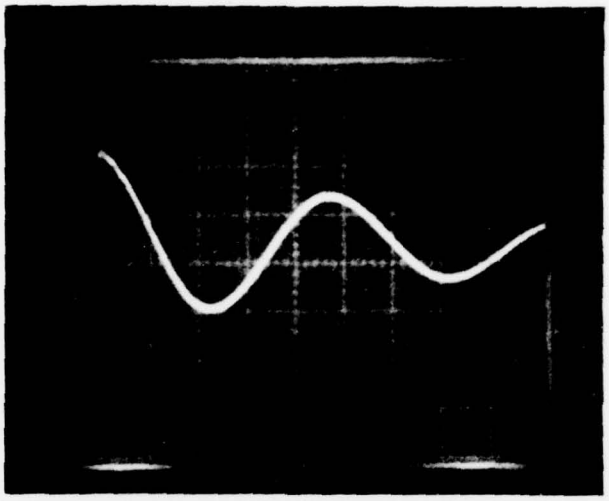

Figure A-4 Voltage at output of Capacitor bank with Carbon block load horizontal-10 μs/div, Vertical 5 KV/div.

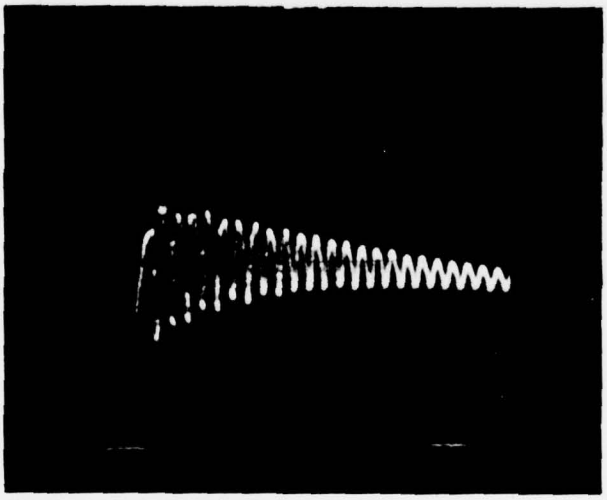

Figure A-5 Voltage at output of Capacitor bank with Carbon block load horizontal-1.0 μs/div, Vertical 5KV/div.